

One-Shot Batch Blind Separation of Delayed Sources

L. M. Leung and M. Vuskovic

Department of Mathematical and Computer Sciences
SDSU, San Diego, CA 92182-7720

Abstract

A one-shot batch algorithm for blind separation of a mixture of delayed source signals is presented. The algorithm has two stages, the sampling stage in which the signals are measured and the required auto and cross-correlation functions are generated, and the optimization stage in which the optimal values of the decorrelator parameters are computed. The decorrelator is based on the second-order FIR filters. The experiments have shown that the batch approach is very robust and time-wise effective in the case of real EMG signals. The paper illustrates the algorithms on the artificially generated signals.

1. Introduction

This work was motivated by an effort to use electro myographic (EMG) signals to interface a human arm and an artificial multifingered robot hand. Four surface EMG electrodes were placed on the human forearm and the measured signals were used to classify intended hand preshaping configuration in an object grasping operation [9], [10]. The possible grasp modes were grouped into four classes: cylindrical, spherical, lateral and precision grasp. The electrode placement was generally determined according to the location of different muscle groups that control thumb, index, middle and little finger. Numerous experiments have shown that the classification hit rate very much depends on the electrode placement and on the cross-talk between some of the electrodes. It is believed that the particular muscles, although they work in an unknown synergetic context, still are statistically independent. Therefore, the blind separation techniques pioneered by [7] and further developed in [4], [1], [2], and many other subsequent publications, which have proposed various approaches for separation of static (instantaneous) mixtures.

In the case of EMGs these techniques have offered some limited success in signal decorrelation. The reason why these techniques weren't fully successful lies in the fact that the signal sources (the

muscles) are embedded in a tissue that is in effect a volume conductor which allows that one surface electrode picks signals from different sources. In addition, the signals propagate through the tissue with a finite speed, thus resulting in a mixture that contains delayed signals. One of the first treatments of the separation of delayed signals was given in [8]. Based on the assumption of delayed mixtures a dynamic decorrelator was proposed in [11], which is conceptually depicted in Figure 1.

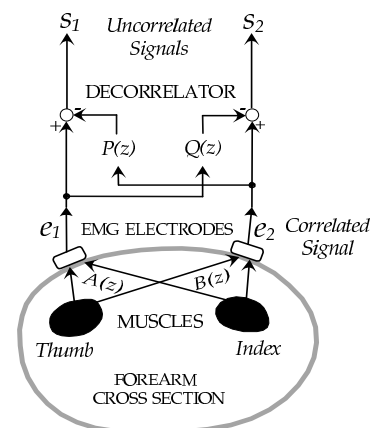


Figure 1: Conceptual representation of signal mixing and signal separation with FIR filters ($A(z)$ and $B(z)$ are mixing filters, while $P(z)$ and $Q(z)$ are decorrelator filters.)

The decorrelation was based on two stationary FIR filters which are discussed in the next section. The dynamic decorrelators have offered surprisingly good results, which are illustrated in Figure 2. The figure compares cross-correlation functions of the measured (dynamically mixed) signals with the cross-correlation functions of the separated signals obtained by using static and dynamic decorrelators. The delayed and convolved mixtures have rapidly gained the attention in last five years and many previously proposed algorithms developed for static mixtures were extended to delayed and convolved mixtures. A good survey of this was given in

[5] and [3].

The separation algorithm in [11] was based on a batch processing approach in which the measured signals are recorded for some period of time in order to acquire their auto and cross-correlation functions, and to compute the associated features for pattern recognition. After that period of time, the optimal parameters of decorrelator filters were computed and used to modify the computed features, to make them uncorrelated. This operation is repeated for each particular prehensile motion (object grasp). Many experiments have shown that the batch approach in this context is more robust and stable than the continuous approach used by most of the researchers. A more detailed presentation of this approach, including some essential improvements are done in [6]. This work summarizes results from [11] and [6]. The effectiveness of the algorithm is shown on two artificially created and mixed signals. The real EMG signals are considered in details in [6].

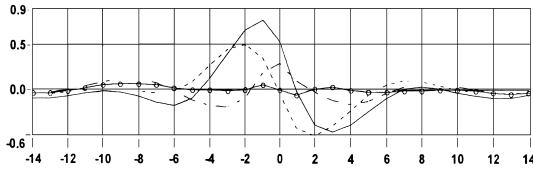


Figure 2: Cross-correlation functions of EMG signals before separation (solid line) and after separation using different filters: dashed line - $P(z) = p_0$ (no delays); broken line - $P(z) = p_0 + p_1z^{-1}$; line with circles - $P(z) = p_0 + p_1z^{-1} + p_2z^{-2}$. ($Q(z)$ has identical structure as $P(z)$).

2. Decorrelation

For the further discussion we suppose two uncorrelated source signals $m_1(t)$ and $m_2(t)$. Their delayed mixture can be written as:

$$\begin{aligned} e_1 &= m_1 + \sum_{k=0}^n a_k m_2(t - k\Delta), \\ e_2 &= m_2 + \sum_{k=0}^n b_k m_1(t - k\Delta). \end{aligned} \quad (1)$$

where a_k and b_k are the unknown mixture coefficients and $e_1(t)$ and $e_2(t)$ are measured signals. After applying z -transform equations (1) become:

$$\begin{aligned} E_1 &= M_1 + A(z)M_2, \\ E_2 &= M_2 + B(z)M_1. \end{aligned} \quad (2)$$

with $A(z) = \sum_{k=0}^n a_k z^{-k}$ and $B(z) = \sum_{k=0}^n b_k z^{-k}$ being the mixture polynomials. The cancellation

of the mixing effect, i.e. the decorrelation, can be achieved by adding two similar polynomials $P(z) = \sum_{k=0}^m p_k z^{-k}$ and $Q(z) = \sum_{k=0}^m q_k z^{-k}$, in an arrangement as shown in Figure 1. The arrangement generates new signals $s_1(t)$ and $s_2(t)$, whose z -transforms are:

$$\begin{aligned} S_1 &= E_1 - P(z)E_2, \\ S_2 &= E_2 - Q(z)E_1. \end{aligned} \quad (3)$$

After substituting (2) into equations (3) the latter become:

$$\begin{aligned} S_1 &= (1 - B(z)P(z))M_1 + (A(z) - P(z))M_2, \\ S_2 &= (B(z) - Q(z))M_1 + (1 - A(z)Q(z))M_2. \end{aligned} \quad (4)$$

Clearly, signals $s_1(t)$ and $s_2(t)$ become uncorrelated if $P(z) = A(z)$ and $Q(z) = B(z)$. Note, the second (permuted) solution, $P(z) = B(z)^{-1}$ and $Q(z) = A(z)^{-1}$ is not feasible if $P(z)$ and $Q(z)$ have a finite order. The uncorrelatedness of signals $s_i(t)$ implies that the cross-correlation function:

$$s_{12}(\tau) = \overline{s_1(t)s_2(t+\tau)} = \frac{1}{2T} \int_{-T}^T s_1(t)s_2(t+\tau)dt, \quad (5)$$

is zero for all τ . In reality the mixing polynomials $A(z)$ and $B(z)$ are not known. Therefore we have to decide about the order m of the decorrelator polynomials $P(z)$ and $Q(z)$ and about the size of the delay interval Δ , then to determine the optimal values of coefficients p_k and q_k , which minimize some measure of $s_{12}(\tau)$. Numerous experiments with real EMG signals [9], [11] have shown that a reasonable order of the decorrelator is $m = 2$. In addition, it was found that the optimal value for delay is $\Delta = 2ms$. This can be seen from typical cross-correlation functions shown on figure 2. As seen the cross-correlation function of the measured signals $e_{12}(\tau)$ has maximums that are at -1 and $+3ms$. The figure also shows the cross-correlation functions $s_{12}(\tau)$ for different m . The case $m = 0$ (no delays) offers very little improvement. Case $m = 1$ shows a significant improvement, while the case $m = 2$ yields almost zero cross-correlation. The experiments have suggested that the further increase of m does not offer any significant improvement over the case $m = 2$, and therefore would not justify the expense of complexity and time overhead for the separation algorithms.

For the minimization criteria we will use the simple mean-square operator:

$$J(p, q) = \overline{s_{12}(\tau)^2} = \int_{-W}^W s_{12}(\tau)^2 d\tau, \quad (6)$$

where the time interval $[-W, W]$, $W < T$, is chosen so that it contains the significant parts of the cross-correlation function. Normally the integration interval W is much smaller than the sampling interval T . For example, in case of EMG signals used in [9] the values were typically $T = 300 \text{ ms}$ and $W = 20 \text{ ms}$.

For the further discussion, we express J explicitly in terms of p and q . Equation (3) can be rewritten for time domain:

$$\begin{aligned} s_1(t) &= e_1(t) - p^T \phi_2(t), \\ s_2(t) &= e_2(t) - q^T \phi_1(t), \end{aligned} \quad (7)$$

where $\phi_1(t) = [e_1(t), e_1(t - \Delta), e_1(t - 2\Delta)]^T$ and $\phi_2(t) = [e_2(t), e_2(t - \Delta), e_2(t - 2\Delta)]^T$ are measured signals and their delays. By applying (5) to (7) follows [6]:

$$s_{12}(\tau) = e_{12}(\tau) - p^T \phi_{22}(\tau) - q^T \phi_{11}(\tau) + p^T \Phi_{21}(\tau)q, \quad (8)$$

$$\begin{aligned} \phi_{11}(\tau) &= [e_{11}(\tau), e_{11}(\tau - \Delta), e_{11}(\tau - 2\Delta)]^T, \\ \phi_{22}(\tau) &= [e_{22}(\tau), e_{22}(\tau + \Delta), e_{22}(\tau + 2\Delta)]^T, \end{aligned} \quad (9)$$

$$\Phi_{21}(\tau) = \begin{bmatrix} e_{21}(\tau) & e_{21}(\tau - \Delta) & e_{21}(\tau - 2\Delta) \\ e_{21}(\tau + \Delta) & e_{21}(\tau) & e_{21}(\tau - \Delta) \\ e_{21}(\tau + \Delta) & e_{21}(\tau + \Delta) & e_{21}(\tau) \end{bmatrix}, \quad (10)$$

where $e_{ij}(\tau)$ are the cross-correlation functions of the measured signals, i.e. $e_{ij}(\tau) = \overline{e_i(t)e_j(t + \tau)}$.

3. Minimization of J

Objective function $J(p, q)$ defined by (6) can be expanded into Taylor series in the vicinity of some point $\tilde{r} = [\tilde{p}^T, \tilde{q}^T]^T$ (the smoothness and differentiability of $J(p, q)$ can be easily verified):

$$J(p, q) = J(\tilde{p}, \tilde{q}) + g(r - \tilde{r}) + (r - \tilde{r})^T H(r - \tilde{r}) + \dots \quad (11)$$

where g and H are the gradient and the Hessian defined as:

$$g = \left[\frac{\partial J}{\partial p}, \frac{\partial J}{\partial q} \right], \quad H = \frac{1}{2} \begin{bmatrix} \frac{\partial^2 J}{\partial p^2} & \frac{\partial^2 J}{\partial p \partial q} \\ \frac{\partial^2 J}{\partial q \partial p} & \frac{\partial^2 J}{\partial q^2} \end{bmatrix} \quad (12)$$

In light of equations (6), (7), and (12), the components of g and H can be expressed in terms of p and q [6]:

$$g(p, q) = \left[\overline{s_{12} u^T}, \overline{s_{12} v^T} \right] \quad (13)$$

$$H(p, q) = \begin{bmatrix} \overline{u u^T} & \overline{u v^T} + \overline{\Phi_{21}^T s_{12}} \\ \overline{v u^T} + \overline{\Phi_{21} s_{12}} & \overline{v v^T} \end{bmatrix}, \quad (14)$$

with:

$$u = -\phi_{22} + \Phi_{21} q, \quad v = -\phi_{11} + \Phi_{21}^T p. \quad (15)$$

The time variable τ of functions $u(\tau)$, $v(\tau)$, $s_{12}(\tau)$, $\phi_{11}(\tau)$, $\phi_{22}(\tau)$, and $\Phi_{21}(\tau)$ is omitted in equations above for the sake of simplicity.

In order to minimize $J(p, q)$ we can employ simple gradient method. However, the practical experience has shown that the gradient method is generally very slow and unstable due to the elliptic behavior of $J(p, q)$. In order to improve the convergency, we can also use the second-order successive approximation technique which uses the Hessian:

$$r_{j+1} = r_j - K H_j^{-1} g_j^T, \quad (16)$$

with a constant gain matrix $K = \text{diag}(k_1, k_2, \dots, k_6)$. The minimization process can be summarized as follows:

1. Acquire signals $e_1(t)$ and $e_2(t)$ (during sampling period T)
2. Compute the cross-correlation functions $e_{11}(\tau)$, $e_{21}(\tau)$, and $e_{22}(\tau)$
3. Set the initial values for p and q (e.g: $p = [0, 0, 0]$, $q = [0, 0, 0]$)
4. Compute $s_{12}(\tau)$, $u(\tau)$ and $v(\tau)$, using equations: (8) and (15)
5. Compute g and H , equations (13) and (14)
6. Compute the new values for p and q , equation (16)
7. If variations of p and q are not sufficiently small go back to step 4.
8. Compute $s_1(t)$ and $s_2(t)$, using equations (7)

It is important to note that the only time-critical operation here is sampling of the measurement data (step 1), which takes time T . The length of T is determined by the sampling rate of the measurement sensor, and by the required number of samples. The computation of the auto and cross-correlation functions (step 2) can be performed during the data acquisition time by using recurrent formulas. Steps 3 through 7 are performed in a negligible short time, depending on the employed computer resources. Generation of the separated signals $s_1(t)$ and $s_2(t)$ (step 8) is performed "post mortem" after the final values of the separation parameters p and q are determined. This induces a time delay

of $T + T_S$, (T_S - is the computation time needed for steps 3 through 8). This delay can be avoided if the first sampling period is used for "training", after which the determined separation parameters can be used for the subsequent signal separation. In that case, the time T_S would be reduced to the amount needed to evaluate the equations (7) only. Of course, the training process can still continue simultaneously with the signal separation, in order to periodically refresh the separation parameters.

The working of the algorithm above is demonstrated on artificially generated signals, a sin wave $m_1(t)$ and a square wave $m_2(t)$ with different frequencies (see Figure 3). The mixed signals $e_1(t)$ and $e_2(t)$ are shown in the same figure.

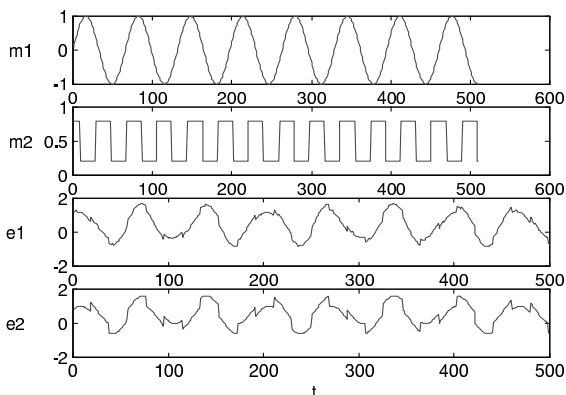


Figure 3: Original signals ($m_1(t)$ and $m_2(t)$) and their convolute mixtures ($e_1(t)$ and $e_2(t)$). The mixing was performed with second-order FIR filters $A(z)$ and $B(z)$.

The separated signals $s_1(t)$ and $s_2(t)$ are shown on Figure 4. As seen, although the cross-correlation function $s_{12}(t)$ was near zero, the square wave signal was not fully recovered. This will be successfully done latter in this paper (see Figure 6).

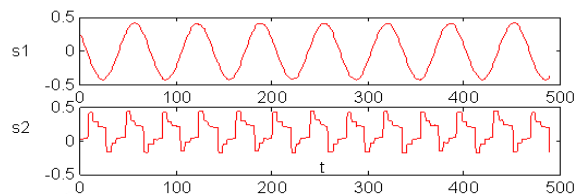


Figure 4: Decorrelated signals obtained after separation

4. The Pseudo Hessian

The convergence of various approaches in minimization of $J(p, q)$ applied to the artificial signals above, is shown in Figure 5. The initial values of decorrelator parameters were chosen: $p = q = [0, 0, 0]^T$. The second-order successive approximation approach was superior in the first iteration over the gradient method. This proved to be a typical case. Unfortunately, the second-order approach didn't perform always as expected. In many occasions it was unstable. The reason is that the Hessian wasn't always positive definite. A short look at the equation (14) reveals the additive terms $\overline{\Phi}_{21}^T s_{12}$ and $\overline{\Phi}_{21} s_{12}$ in the off-diagonal sub matrices of the Hessian. These terms can contribute to the departure from the positive definiteness. Therefore, these terms were removed heuristically, thus creating a "pseudo Hessian". The pseudo Hessian approach gave surprisingly good results. The diagram in Figure 5 shows that the pseudo Hessian approach has completed the optimization after first iteration. The behavior of this approach was extremely good in the vicinity of the minimum of J , which was not the case with the other approaches. This behavior was consistent in many experiments performed on artificial signals and on real-life EMG signals as well.

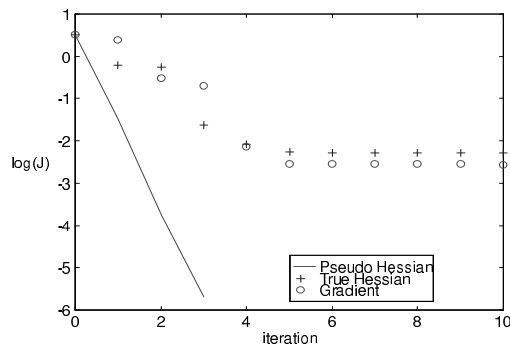


Figure 5: Minimization of J using different algorithms: gradient approach (circles); successive quadratic approximations with exact Hessian (pluses), and with pseudo-Hessian (solid line). The latter approach was able to sufficiently minimize J in a single iteration. The initial value of J was 3.224.

5. One-Shot Minimization

The usage of the pseudo Hessian makes the single iteration in the minimization of J sufficient. This simplifies significantly the separation algorithm. In addition, usage of zero initial values for the decorrelator parameters p and q , the algorithm simplifies

even more: the entire process now reduces to the following three equations:

$$g_o = \begin{bmatrix} \overline{\overline{-e_{12} \phi_{22}^T}} & \overline{\overline{e_{12} \phi_{11}^T}} \\ \overline{\overline{\phi_{22} \phi_{22}^T}} & \overline{\overline{\phi_{22} \phi_{11}^T}} \\ \overline{\overline{\phi_{11} \phi_{22}^T}} & \overline{\overline{\phi_{11} \phi_{11}^T}} \end{bmatrix} \quad (17)$$

$$\begin{bmatrix} p \\ q \end{bmatrix} = -H_o^{-1} g_o^T$$

All components in the equations above depend now only on the measured signals $e_i(t)$. The auto-correlation functions $e_{11}(\tau)$ and $e_{22}(\tau)$, and the cross-correlation function $e_{21}(\tau)$, which are elements of ϕ_{22} and ϕ_{22} , can be computed recurrently, and they are all available at the end of the sampling period T .

6. Compensation

If we assume $P(z) = A(z)$ and $Q(z) = B(x)$, the equations (4) become:

$$S_i = (1 - P(z)Q(z))M_i, \quad i = 1, 2 \quad (18)$$

The signals $s_1(t)$ and $s_2(t)$ are uncorrelated, however they are not equal to the unmixed signals $m_1(t)$ and $m_2(t)$. That explains the poor shape of the separated signals in Figure 4. In order to obtain signals that are close to the unmixed signals, we need to solve the equations (18) in the time domain.

By multiplying the polynomials $P(z)$ and $Q(z)$ and by some rearrangements of the equations [6] we get:

$$C_i = S_i/d_0 + (d_1 z^{-1} + d_2 z^{-2} + d_3 z^{-3} + d_4 z^{-4}) C_i, \quad (19)$$

where:

$$\begin{aligned} d_0 &= 1 - p_0 q_0, \\ d_1 &= (p_0 q_1 + p_1 q_0)/d_0, \\ d_2 &= (p_0 q_2 + p_1 q_1 + p_2 q_0)/d_0, \\ d_3 &= (p_1 q_2 + p_2 q_1)/d_0, \\ d_4 &= (p_2 q_2)/d_0. \end{aligned} \quad (20)$$

Note that the symbol M_i is replaced by C_i in order to conceptually distinguish between the truly

unknown original signals $m_i(t)$ and their approximate compensated versions $c_i(t)$.

The time domain version of (19) is:

$$c_i(t) = s_i(t)/d_0 + d_1 c_i(t - \Delta) + d_2 c_i(t - 2\Delta) + d_3 c_i(t - 3\Delta) + d_4 c_i(t - 4\Delta). \quad (21)$$

The compensated version $c_i(t)$ of signals $s_i(t)$ is shown on Figure 6. The signal is almost fully recovered.

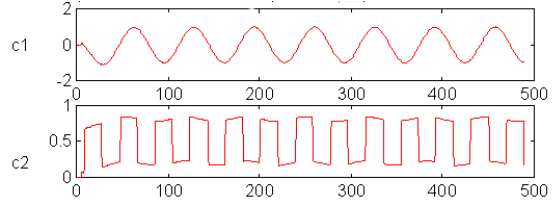


Figure 6: Signals after compensation.

7. Feature Separation

In most cases signals are used for some kind of pattern recognition. For example multi-channel surface EMG signals are recorded from the human forearm in order to control an artificial multifingered hand [9]. For that purpose various EMG patterns that correspond to various grasp modes (cylindric, spherical, lateral or precision grasp) are classified, so that the hand can be properly preshaped by the hand controller for a grasping action. Similarly, the EMG signals can be used to diagnose certain patient's conditions. The signal separation in these situations is necessary in order to minimize the cross-talk between multiple EMG electrodes and to compensate for variations in electrode placements. In addition, the separation can eliminate unwanted artifacts. Before the raw signals are used for classification, they should go through a stage called *feature extraction*. The simplest and perhaps the most useful feature extraction is done by simple integral-of-square method. This applied to the measured signals $e_i(t)$ would give the following definition of features:

$$f_{e_i} = \int_0^{T_F} e_i(t)^2 dt. \quad (22)$$

Similarly, the features extracted from the separated signals $s_i(t)$ would be:

$$f_{s_i} = \int_0^{T_F} s_i(t)^2 dt \quad (23)$$

The integration interval T_F isn't necessarily equal to the sampling period, but is normally close, which means that the computation of features involves squaring and summing up of hundreds or thousands of samples. Consequently, the total time to extract the features would be $T + T_S + T_F$, where T_S is the computation time needed to determine decorrelator parameters p and q , while T_F is the time to compute the features. The sampling time T is unavoidably long and can not be decreased by using faster computers, which is the case with other two time intervals. As mentioned in section 3., signal separation can be overlapped with the sampling process by using recurrent formulas for auto and cross-correlation functions. This would greatly reduce T_S . Similarly, the feature extraction time can also be saved by overlapping the feature extraction with the sampling process, therefore eliminating T_F almost entirely. This is possible in case of the simple feature extraction method (22) and (23).

Substitution of equations (7) and (22) into (23) gives:

$$\begin{aligned} f_{s_1} &= f_{e_1} + p^T \omega_{12} + p^T \Omega_2 p, \\ f_{s_2} &= f_{e_2} + q^T \omega_{21} + q^T \Omega_1 q, \end{aligned} \quad (24)$$

where:

$$\omega_{ij} = -2 \int_0^{T_F} e_i(t) \phi_j(t) dt, \quad \Omega_i = \int_0^{T_F} \phi_i(t) \phi_i(t)^T dt.$$

Provided that the values of ω_{12} and Ω_i are computed during the sampling period T , all what is left to do after the decorrelator parameters are determined, is to perform a couple of multiplications and additions in (24).

8. Conclusion

A one-shot batch algorithm for blind separation of delayed mixture of two signals is presented. The algorithm has proven to be very robust and effective for real EMG signals. The concepts and the effectiveness of the algorithm is illustrated on two artificially generated and mixed signals. Future work will be focussed on the separation of several simultaneous signals including noise.

References

[1] S. Amari, A. Cichocki and H.H. Yang, "Recurrent Neural Networks for Blind Separation of Sources," *Ibid*, pp. 37-42, 1995.

[2] A.J. Bell and T.J. Sejnowski, "An Information Maximization Approach to Blind Separation and Blind Deconvolution," *Neural Computation*, Vol. 7, No. 6, pp. 1004-1034, 1995.

[3] T.W. Lee, A.J. Bell and R. Lambert, "Blind Separation of Convolved and Delayed Sources," *Advances in Neural Information Processing Systems* 9, pp. 758-764, 1996.

[4] P. Comon, "Independent Component Analysis, A New Concept?" *Signal Processing*, Vol. 39, pp. 287-314, 1994.

[5] A. Cichocki, S. Amari and J. Cao, "Neural Network Models for Blind Separation of Time Delayed and Convolved Signals," *IECE Trans. Fundamentals*, Vol. E80-A, No. 9, pp. 1595-1603, September 1997.

[6] L.M. Leung, "Blind Separation of Surface EMG Signals," MS Thesis, Dept. of Mathematical and Computer Sciences, SDSU, October 10, 1999.

[7] C. Jutten and J. Harault, "Blind Separation of Sources, Part I: An Adaptive Algorithm based on Neuromimetic Architecture," *Signal Processing*, Vol 24, pp. 1-10, 1991.

[8] J.C. Platt and F. Faggin, "Networks for the Separation of Sources that are Superimposed and Delayed," in: "Advances in Neural Processing Systems 4," Ed. by J.E. Moody, S.J. Hanson and R.P. Lipmann, pp. 730-737, Morgan Kaufmann Publishers, San Mateo, California, 1991.

[9] M.I. Vuskovic, A.L. Pozos and R. Pozos, "Classification of Grasp Modes Based on Electromyographic Patterns of Preshaping Motion," *Int. IEEE Conf. on SMC*, October 1995, Vancouver, pp. 89-95, 1995.

[10] M.I. Vuskovic, J. Schmit, B. Dundon and C. Konopka, "Hierarchical Discrimination of Grasp Modes Using Surface EMGs," *Proc. of the 1996 IEEE Internat. Conference on Robotics and Automation*, Minneapolis, Minnesota, April 1996.

[11] M.I. Vuskovic and X. Li, "Blind Separation of Surface EMG Signals," *Proc. of the 18th Annual International Conference of the IEEE Engineering in Medicine and Biology Society*, Amsterdam, the Netherlands, October 31-November 3, 1996.